TẠP CHÍ KHOA HỌC
TRƯỜNG ĐẠI HỌC SƯ PHẠM TP HỒ CHÍ MINH
Tập 21, Số 3 (2024): 424-432
Website: https://journal.hcmue.edu.vn
ISSN: 2734-9918

HO CHI MINH CITY UNIVERSITY OF EDUCATION
JOURNAL OF SCIENCE
Vol. 21, No. 3 (2024): 424-432
https://doi.org/10.54607/hcmue.js.21.3.4110(2024)

Research Article

ANALYSIS OF E1 TRANSITION IN PD RADIATIVE CAPTURE WITHIN POTENTIAL MODEL

Dao Nhut Anh*, Do Huy Tho, Nguyen T. Hue, Hoang Thai An
Ho Chi Minh City University of Education, Vietnam
Corresponding author: Dao Nhut Anh – Email: daonhutanh2004@gmail.com
Received: January 19, 2024; Revised: February 28, 2024; Accepted: February 28, 2024

ABSTRACT

The proton-deuteron (pd) radiative capture reaction significantly impacts primordial nucleosynthesis. Employing a phenomenological potential model, we analyze pd radiative capture at energies below 300 keV, emphasizing electric dipole (E1) transitions. Bound and scattering states are exclusively determined through the Woods-Saxon potential by solving Schrödinger equations. The selected experimental data were used to validate the proposed theoretical framework.

Keywords: potential model; proton-deuteron; radiative capture

1. Introduction

Primordial nucleosynthesis, also known as Big Bang nucleosynthesis (BBN), is a pivotal astrophysical process occurring in the early stages of the universe. It entails the synthesis of nuclei beyond the lightest hydrogen isotope, contributing to the formation of various elements in the cosmos. This nucleosynthesis unfolds in the initial moments following the Big Bang.

The *pd* radiative capture or $d(p,\gamma)^3$He reaction, a fusion of deuteron and proton, plays a crucial role in BBN as a nuclear fusion pathway. In this process, deuterium and a proton combine to form ^{3}He, accompanied by the emission of a γ-ray photon. This reaction is part of the complex network of nuclear reactions during BBN, influencing the abundance of ^{3}He and the overall primordial element abundance pattern. The investigation extensively reviews related literature both empirically and theoretically on astrophysical *S* factors related to solar fusion reactions (Adelberger et al., 2011).

Experimental measurements of this reaction at low energy have been conducted in various accelerator experiments (Bystritsky et al., 2008; Casella et al., 2002; Griffiths et al., 1963; Mossa et al., 2020; Schmid et al., 1995; Tišma et al., 2019; Turkat et al., 2021). However, these measurements come with considerable uncertainties, impacting the comparison between predicted and observed primordial abundances.

Cite this article as: Dao Nhut Anh, Do Huy Tho, Nguyen T. Hue, & Hoang Thai An (2024). Analysis of E1 transition in pd radiative capture within potential model. *Ho Chi Minh City University of Education Journal of Science, 21*(3), 424-432.

Theories of *pd* radiative capture and scattering have a long history, employing advanced techniques (Friar et al., 1991; Kievsky et al.,1995; Marcucci et al., 2016; Viviani et al., 1996). In this work, we adopt a phenomenological approach (Huang et al., 2010; Xu et al., 2013) to investigate this reaction, aiming to obtain astrophysical *S* factors and the extrapolated value of $S_{E1}(0)$. Radial overlap wave functions for both bound and scattering states are crucial inputs for the potential model. The Woods-Saxon potentials for the nuclear part are used in the present work. These wave functions are obtained by solving Schrödinger equations for both states. The *S* factor calculation for *pd* radiative capture is then compared to experimental data, focusing on the *E*1 transition below 300 keV.

The forthcoming section will detail the formalism of the potential model for *pd* radiative capture, taking into account the *E*1 transition. The results and ensuing discussions will be presented in Section 3, followed by conclusions in Section 4.

2. Potential model for radiative capture reaction

2.1. Electric dipole transition in radiative capture

The astrophysical *S* factor for the *E*1 transition is defined as

$$S_{E1}(E) = \sigma_{E1}(E) E e^{2\pi\eta}, \tag{1}$$

where η is the Sommerfeld parameter. The cross-section for the *E*1 transition to a bound state is now written as

$$\sigma_{E1}(E) = \frac{16\pi}{9}\frac{k_\gamma^3}{\hbar\nu}\frac{1}{(2s_p+1)(2I_d+1)}\sum_{\ell_s j_s J_s} |M_{E1}(E)|^2, \tag{2}$$

where $\hbar$ is the reduced Planck constant, k_γ is the photon wave number as a function of the proton energy *E*, and ν is the relative velocity of the proton-deuteron system. The intrinsic spins s_p and I_d are of the proton and deuteron, respectively. The reduced matrix elements of the *E*1 transition are written as

$$M_{E1} = \left\langle \left[I_d \otimes (\ell_b \otimes s_p)_{j_b} \right]_{J_b} \| O_{E1} \| \left[I_d \otimes (\ell_s \otimes s_p)_{j_s} \right]_{J_s} \right\rangle, \tag{3}$$

where the scattering state is $\left| \left[I_d \otimes (\ell_s \otimes s_p)_{j_s} \right]_{J_s} \right\rangle$ and the bound state is $\left| \left[I_d \otimes (\ell_b \otimes s_p)_{j_b} \right]_{J_b} \right\rangle$. Both states are sandwiched by the electric dipole operator O_{E1} (Xu et al., 2013). The M_{E1} can be simplified by the calculation of the single-particle reduced matrix element.

$$M_{E1} = C_e (-1)^{I_d + j_b + J_s + 1} \hat{J}_s \hat{J}_b \begin{Bmatrix} j_b & J_b & I_d \\ J_s & j_s & 1 \end{Bmatrix} M_{E1}^{(\text{s.p.})}, \tag{4}$$

where the hat notation is $\hat{J} = \sqrt{2J+1}$ and the curly bracket is the Wigner 6*j* coefficient, and C_e represents the effective charge. The single-particle reduced matrix elements $M_{E1}^{(\text{s.p.})}$ can be written as

$$M_{E1}^{(\text{s.p.})} = \sqrt{\frac{3}{4\pi}}\hat{\ell}_s \hat{j}_s \hat{j}_b (\ell_s 010 | \ell_b 0) \begin{Bmatrix} \ell_s & 1/2 & j_s \\ j_b & 1 & \ell_b \end{Bmatrix} \cdot I_{E1}, \tag{5}$$

where the round bracket component is the Clebsch-Gordan coefficient. The radial overlap integral of two states, which plays the most crucial role in the potential model calculation, is given by

$$I_{E1} = \int dr \phi_{n\ell_b j_b}(r) r \chi_{\ell_s j_s}(E, r), \tag{6}$$

where $\chi_{\ell_s j_s}$ and $\phi_{n\ell_b j_b}$ are the wave functions of the scattering state and bound state, respectively.

2.2. Bound and scattering equations

The wave functions for bound and scattering states are solutions to the radial Schrödinger equations, each corresponding to a specific single-particle wave function. The equations governing these states are given by

$$\left[-\frac{\hbar^2}{2\mu}\frac{d^2}{dr^2} + V_b(r) \right] \phi_{n\ell_b j_b}(r) = E_b \phi_{n\ell_b j_b}(r), \tag{7}$$

$$\left[-\frac{\hbar^2}{2\mu}\frac{d^2}{dr^2} + V_s(r) \right] \chi_{\ell_s j_s}(E, r) = E \chi_{\ell_s j_s}(E, r), \tag{8}$$

where μ represents the reduced mass, and the binding energies $E_b < 0$ are discrete, while the scattering energies $E > 0$ are continuous. The potentials for both scattering and bound states include contributions from nuclear, Coulomb, and centrifugal terms

$$V(r) = V_{\text{nucl.}}(r) + V_{\text{Coul.}}(r) + V_{\text{cent.}}(r). \tag{9}$$

The nuclear part takes the form of a Woods-Saxon potential

$$V_{\text{nucl.}}(r) = \frac{V_0}{1 + e^{(r-R)/a}}, \tag{10}$$

where R and a are the radius and diffuseness parameters of the Woods-Saxon potentials, respectively. The depth of potential $V_0 < 0$ is adjusted to match experimental data. The Coulomb potential is described by a spherically symmetric uniformly charged sphere

$$V_{\text{Coul.}}(r) = \begin{cases} \dfrac{Ze^2}{r}, & r \geq R_{\text{C}} \\ \dfrac{Ze^2}{2R_{\text{C}}}\left(3 - \dfrac{r^2}{R_{\text{C}}^2}\right), & r < R_{\text{C}} \end{cases}, \tag{11}$$

where R_{C} is the Coulomb radius, and, in this work, we set $R_{\text{C}} = R$. As the $E1$ transition involves different orbital angular momenta $\ell_b \neq \ell_s (\Delta\ell = \pm 1)$, the centrifugal term differs between scattering and bound states

$$V^{s}_{\text{cent.}}(r)=\frac{\hbar^2}{2\mu}\frac{\ell_s(\ell_s+1)}{r^2},\ V^{b}_{\text{cent.}}(r)=\frac{\hbar^2}{2\mu}\frac{\ell_b(\ell_b+1)}{r^2}. \quad (12)$$

3. Results and discussions

In this analysis, we focus on $E1$ transitions to the ground state of ^{3}He with $J_b=1/2$. The ground state of ^{3}He is modeled as a proton with spin $s_p=1/2$ coupled to the deuterium core, having an intrinsic spin $I_d=1$. We fit the Woods-Saxon potential to match the form of the Hartree-Fock potential with the SLy5 force, determining the parameters R = 2.31 fm and a = 0.37 fm through fitting as shown in Figure 1. The depth V_0 is the sole parameter adjusted to simultaneously reproduce the binding energy and *pd* scattering.

Table 1. *Relevant single-particle states in the E1 transition within the potential model*

No.	$\ell_s j_s$	J_s	$\ell_b j_b$	J_b	s_p	I_d
1	$p_{1/2}$	1/2	$s_{1/2}$	1/2	1/2	1
2	$p_{1/2}$	3/2	$s_{1/2}$	1/2	1/2	1
3	$p_{3/2}$	1/2	$s_{1/2}$	1/2	1/2	1
4	$p_{3/2}$	3/2	$s_{1/2}$	1/2	1/2	1

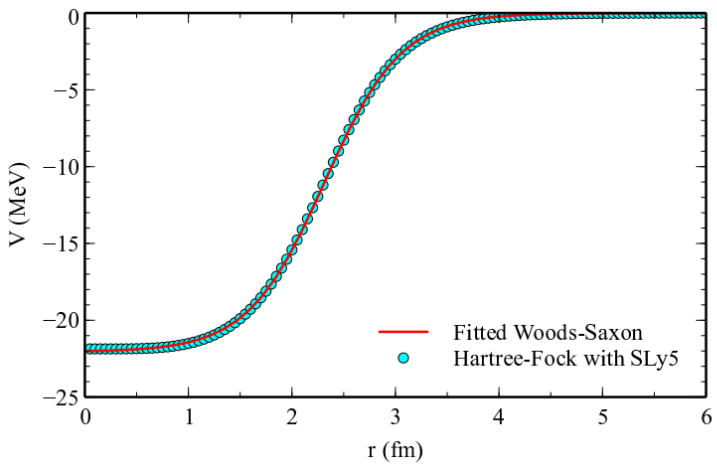

Figure 1. *The Woods-Saxon potential with $V_0 = -22$ MeV, R = 2.31 fm and a = 0.37 fm obtained from fitting to the converged Hartree-Fock potential with SLy5*

In the potential model, a proton is captured into the $1s_{1/2}$ state ($\ell_b=0$) from incoming p states ($\ell_s=1$). The binding energy of the $1s_{1/2}$ proton equals the Q value of the reaction, given as $E_b=-5.5$ MeV. To achieve this binding energy, we utilize $V_0=-32.06$ MeV. The single-particle states involved in the $E1$ transition are presented in Table 1. The squared asymptotic normalization constant for the bound s state of ^{3}He is determined to be 3.18 in this study. The experimental values are found to be 3.4 ± 0.2 (Plattner et al., 1977) and 3.5 ± 0.4 (Bornand et al., 1978).

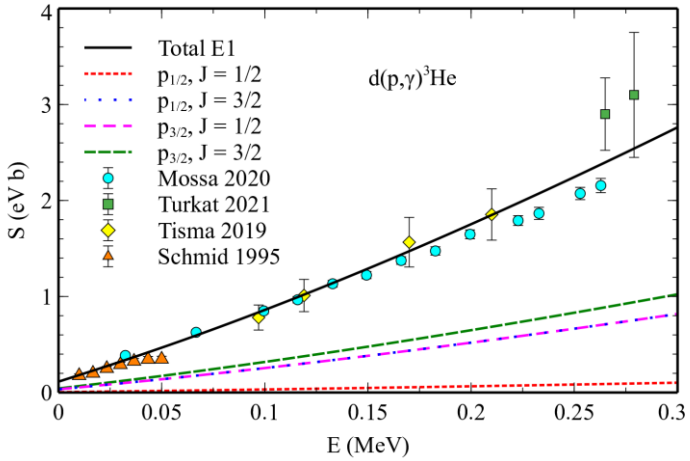

Figure 2. *Astrophysical S factor with only E1 transition of d(p, γ)^{3}He reaction compared with the experimental data from previous studies*

(Mossa et al., 2020; Schmid et al., 1997; Tišma et al., 2019; Turkat et al., 2021).

Figure 2 displays the calculated astrophysical S factor for the $d(p,\gamma)^3$He reaction, considering only $E1$ transitions below 300 keV. Notably, the calculated curve aligns well with experimental data from previous studies (Mossa et al., 2020; Schmid et al., 1997; Tišma et al., 2019; Turkat et al., 2021). Notably, the largest magnitude of the transition occurs for the incoming $p_{3/2}$ wave with $J=1/2$ (depicted by the magenta dashed line), while the contribution of the $p_{1/2}$ wave with $J=1/2$ (represented by the red dotted line) is negligible. The magnitudes of $p_{1/2}$ with $J=3/2$ and $p_{3/2}$ with $J=1/2$ are equal due to the omission of spin-orbit splitting.

The statistical method χ^2 is employed to evaluate the goodness of fit between observed (experimental) data and expected (theoretical) values. The χ^2 values are determined by

$$\chi^2=\frac{1}{N}\sum_{i=1}^{N}\left(\frac{S_i^{\text{exp}}-S_i^{\text{theo}}}{\sigma_i}\right)^2, \tag{13}$$

where S_i^{exp} and S_i^{theo} represent experimental and theoretical values, respectively. The uncertainties (errors) σ_i are associated with the N measured data points. For the experimental data below 300 keV reported in the literature review (Mossa et al., 2020; Schmid et al., 1997; Tišma et al., 2019; Turkat et al., 2021) with 26 data points, the calculated χ^2 is 3.78.

Extending the data points up to 1 MeV (36 data points from Mossa et al., 2020; Schmid et al., 1997; Tišma et al., 2019; Turkat et al., 2021) and using $V_0=-32$ MeV, the extracted χ^2 value is 4.24. Figure 3 illustrates the variations in the chi-squared values when altering the depths of the scattering potentials. The minimum χ^2 value is found at $V_0=-27.3$ MeV.

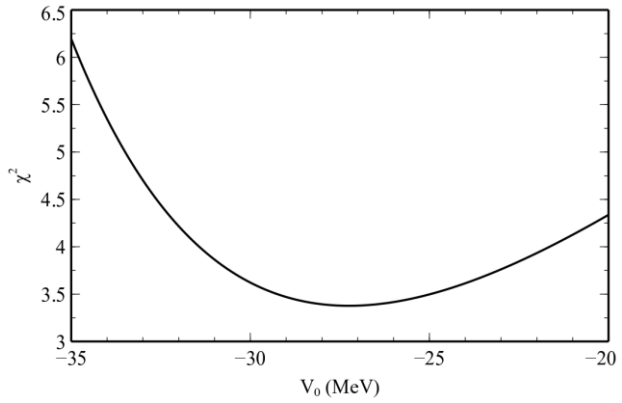

Figure 3. *Comparison of χ^2 values obtained from the astrophysical S factor calculation and experimental data for the $d(p,\gamma)^3$He reaction. The test includes data points up to 1 MeV with the variation of V_0 from −35 MeV to −25 MeV*

Figure 4 shows the total *S* factor of *pd* radiative capture when comparing the cases of using $V_0 = -32$ MeV and $V_0 = -27$ MeV. The case with $V_0 = -27$ MeV is in better agreement with the recently measured experimental data reported by Mossa et al. (2020). Additionally, it exhibits a smaller slope in comparison to the other case. The extrapolated values at extremely low energy do not differ significantly between these cases.

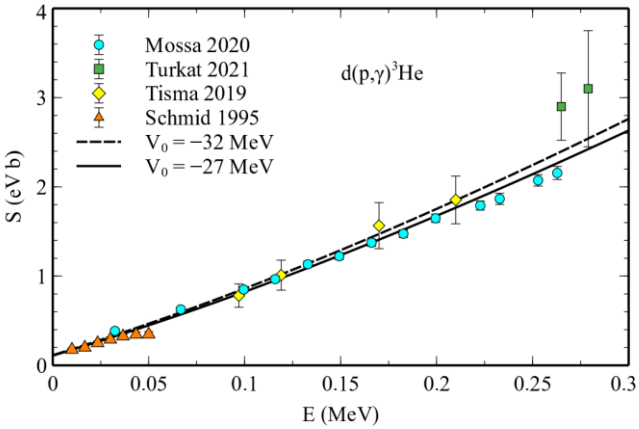

Figure 4. *Astrophysical S factor with only E1 transition of $d(p,\gamma)^3$He reaction using $V_0 = -32$ MeV (dashed line) and $V_0 = -27$ MeV (solid line) vs. data from Mossa et al. (2020), Schmid et al. (1997), Tišma et al. (2019), and Turkat et al. (2021)*

The extrapolated values of $S_{E1}(0)$, considering the *E*1 contribution, are determined to be 0.115 eV b for $V_0 = -32$ MeV and 0.110 eV b for $V_0 = -27$ MeV in this work. In comparison with the studies by Descouvemont et al. (2004) using *R*-matrix analysis to be $S_{E1}(0) = 0.089 \pm 0.004$ eV b and by Dubovichenko et al. (2020) adopting the modified potential cluster model to be $S_{E1}(0) = 0.135$ eV b. Schmid et al. (1995) using the angular distribution data reported $S_{E1}(0) = 0.053 \pm 0.005$ eV b, and the value for the *p*-wave

component of the zero-energy astrophysical S factor is $S_{E1}(0) = 0.073 \pm 0.007$ eV b (Schmid et al., 1997).

In this study, the astrophysical $S_{E1}(E)$ factor, calculated for energies below 300 keV, is approximated using a cubic function

$$S_{E1}(E) = 0.110 + 6.37E + 8.35E^2 - 5.22E^3, \text{ for } V_0 = -27 \text{ MeV}, \quad (14)$$

where $S_{E1}(E)$ and E are in eV b and MeV, respectively. The polynomial in Eq. (14) is valuable in astrophysical models that simulate the conditions within stars, helping astrophysicists gain insights into the nucleosynthesis processes, energy generation, and overall stellar evolution. It is noteworthy that the best-fit total S factor used in Mossa et al. (2020) was determined as $S(E) = 0.2121 + 5.973E + 5.449E^2 - 1.656E^3$. Comparing the slopes, our $S(E)$ slope, the coefficient of the first derivative $S'(0)$ is close to that reported by Mossa et al. (2020). This positive slope indicates $E1$ resonance behavior at higher energies attributed to p waves. Furthermore, $S_{E1}(0)$ is lower than total $S(0)$, suggesting the influence of the $M1$ transition, a factor not being considered in this study.

4. Conclusions

This study highlights the effectiveness of computing S factors using the potential model, proving to be a valuable tool for investigating radiative capture reactions. The potential model, often considered simple, emerges as an effective approach for describing few-body problems at low energy.

Future work will focus on exploring the role of magnetic dipole ($M1$) transitions, known contributors to enhanced S factors at very low energies. Additionally, the investigations in this study will extend to examining the consistency between *pd* elastic scattering and radiative capture, contributing to a more comprehensive understanding of these complex nuclear processes.

❖ ***Conflict of Interest:*** *Authors have no conflict of interest to declare.*

❖ ***Acknowledgement:*** *This research is funded by Ho Chi Minh City University of Education Foundation for Science and Technology under grant number CS.2023.19.57. We thank N.L.Anh for providing the numerical calculation of the cross-section.*

REFERENCES

Adelberger, E. G., García, A., Hamish Robertson, R. G., Snover, K. A., Balantekin, A. B., Heeger, K., Ramsey-Musolf, M. J., Bemmerer, D., Junghans, A., Bertulani, C. A., Chen, J. -W., Costantini, H., Prati, P., Couder, M., Uberseder, E., Wiescher, M., Cyburt, R., Davids, B., Freedman, S. J., … Typel, S. (2011). Solar fusion cross sections. II. The pp chain and CNO cycles. *Reviews of Modern Physics*, *83*(1), 195-245. https://doi.org/10.1103/RevModPhys.83.195

Bornand, M. P., Plattner, G. R., Viollier, R. D., & Alder, K. (1978). Coupling constants for several light nuclei from a dispersion analysis of nucleon and deuteron scattering amplitudes. *Nuclear Physics A, 294*(3), 492-512. https://doi.org/10.1016/0375-9474(78)90233-6

Bystritsky, V., Gerasimov, V., Krylov, A., Parzhitskii, S., Dudkin, G., Kaminskii, V., Nechaev, B. A., Padalko, V. N., Petrov, A. V., Mesyats, G. A., Filipowicz, M., Wozniak, J., & Bystritskii, V. M. (2008). Study of the pd reaction in the astrophysical energy region using the Hall accelerator. *Nuclear Instruments and Methods in Physics Research Section A: Accelerators, Spectrometers, Detectors and Associated Equipment, 595*(3), 543-548. https://doi.org/10.1016/j.nima.2008.07.152

Casella, C., Costantini, H., Lemut, A., Limata, B., Bonetti, R., Broggini, C., Campajola, L., Corvisiero, P., Cruz, J., D'Onofrio, A., Formicola, A., Fülöp, Z., Gervino, G., Gialanella, L., Guglielmetti, A., Gustavino, C., Gyurky, G., Imbriani, G., Jesus, A. P., … Zavatarelli, S. (2002). First measurement of the d(p,γ)3He cross section down to the solar Gamow peak. *Nuclear Physics A, 706*(1-2), 203-216. https://doi.org/10.1016/S0375-9474(02)00749-2

Descouvemont, P., Adahchour, A., Angulo, C., Coc, A., & Vangioni-Flam, E. (2004). Compilation and R-matrix analysis of Big Bang nuclear reaction rates. *Atomic Data and Nuclear Data Tables, 88*(1), 203-236. https://doi.org/10.1016/j.adt.2004.08.001

Dubovichenko, S. B., Chechin, L. M., Burkova, N. A., Dzhazairov-Kakhramanov, A. V., Omarov, C. T., Nurakhmetova, S. Z., Beisenov, B. U., Ertaiuly, A., & Eleusheva, B. (2020). Rate of Radiative p2H Capture. *Russian Physics Journal, 63*, 1118-1125. https://doi.org/10.1007/s11182-020-02170-9

Friar, J. L., Gibson, B. F., Jean, H. C., & Payne, G. L. (1991). Nuclear transition rates in μ-catalyzed p-d fusion. *Physical Review Letters, 66*(14), 1827-1830. https://doi.org/10.1103/PhysRevLett.66.1827

Griffiths, G. M., Lal, M., & Scarfe, C. D. (1963). The reaction d(p, γ)3He below 50 KeV. *Canadian Journal of Physics, 41*(5), 724-736. https://doi.org/10.1139/p63-077

Huang, J. T., Bertulani, C. A., & Guimaraes, V. (2010). Radiative capture of nucleons at astrophysical energies with single-particle states. *Atomic Data and Nuclear Data Tables, 96*(6), 824-847. https://doi.org/10.1016/j.adt.2010.06.004

Kievsky, A., Viviani, M., & Rosati, S. (1995). Cross section, polarization observables, and phase-shift parameters in p-d and n-d elastic scattering. *Physical Review C, 52*(1), R15-R19. https://doi.org/10.1103/PhysRevC.52.R15

Marcucci, L. E., Mangano, G., Kievsky, A., & Viviani, M. (2016). Implication of the proton-deuteron radiative capture for Big Bang Nucleosynthesis. *Physical Review Letters, 116*(10), Article 102501. https://doi.org/10.1103/PhysRevLett.116.102501

Mossa, V., Stöckel, K., Cavanna, F., Ferraro, F., Aliotta, M., Barile, F., Bemmerer, D., Best, A., Boeltzig, A., Broggini, C., Bruno, C. G., Caciolli, A., Chillery, T., Ciani, G. F., Corvisiero, P., Csedreki, L., Davinson, T., Depalo, R., Di Leva, A.,… Zavatarelli, S. (2020). The baryon density of the Universe from an improved rate of deuterium burning. *Nature, 587*(7833), 210-213. https://doi.org/10.1038/s41586-020-2878-4

Plattner, G. R., Bornand, M., & Viollier, R. D. (1977). Accurate Determination of the He 3-dp and He 3-d*p Coupling Constants. *Physical Review Letters, 39*(3), 127-130. https://doi.org/10.1103/PhysRevLett.39.127

Schmid, G. J., Chasteler, R. M., Laymon, C. M., Weller, H. R., Prior, R. M., & Tilley, D. R. (1995). Polarized proton capture by deuterium and the 2H(p,γ)3He. *Physical Review C, 52*(4), R1732-R1735. https://doi.org/10.1103/PhysRevC.52.R1732

Schmid, G. J., Rice, B. J., Chasteler, R. M., Godwin, M. A., Kiang, G. C., Kiang, L. L., Laymon, C. M., Prior, R. M., Tilley, D. R., & Weller, H. R. (1997). The 2H(p,γ)3He and 1H(d,γ)3He reactions below 80 keV. *Physical Review C, 56*(5), 2565-2581. https://doi.org/10.1103/PhysRevC.56.2565

Tišma, I., Lipoglavšek, M., Mihovilovič, M., Markelj, S., Vencelj, M., & Vesić, J. (2019). Experimental cross section and angular distribution of the 2H(p, γ)3He reaction at Big-Bang nucleosynthesis energies. *The European Physical Journal A, 55*(8), Article 137. https://doi.org/10.1140/epja/i2019-12816-1

Turkat, S., Hammer, S., Masha, E., Akhmadaliev, S., Bemmerer, D., Grieger, M., Hensel, T., Julin, J., Koppitz, M., Ludwig, F., Möckel, C., Reinicke, S., Schwengner, R., Stöckel, K., Szücs, T., Wagner, L., & Zuber, K. (2021). Measurement of the 2H(p,γ)3He S factor at 265–1094 keV. *Physical Review C, 103*(4), Article 045805. https://doi.org/10.1103/PhysRevC.103.045805

Viviani, M., Schiavilla, R., & Kievsky, A. (1996). Theoretical study of the radiative capture reactions 2H(n,γ)3H and 2H(p,γ)3He at low energies. *Physical Review C, 54*(2), 534-553. https://doi.org/10.1103/PhysRevC.54.534

Xu, Y. A., Takahashi, K., Goriely, S., Arnould, M., Ohta, M., & Utsunomiya, H. (2013). NACRE II: an update of the NACRE compilation of charged-particle-induced thermonuclear reaction rates for nuclei with mass number A<16. *Nuclear Physics A, 918,* 61-169. https://doi.org/10.1016/j.nuclphysa.2013.09.007

PHÂN TÍCH DỊCH CHUYỂN E1 TRONG PHẢN ỨNG BẮT PD TRONG KHUÔN KHỔ MÔ HÌNH THẾ

Đào Nhựt Anh*, Đỗ Huy Thọ, Nguyễn T. Huệ , Hoàng Thái An

Trường Đại học Sư phạm Thành phố Hồ Chí Minh, Việt Nam

Tác giả liên hệ: Đào Nhựt Anh - Email: daonhutanh2004@gmail.com

Ngày nhận bài: 19-01-2024; ngày nhận bài sửa: 28-02-2024; ngày duyệt đăng: 28-02-2024

TÓM TẮT

Phản ứng bắt xạ proton-deuteron (pd) ảnh hưởng đáng kể đến quá trình tổng hợp hạt nhân nguyên thủy. Sử dụng mô hình thế hiện tượng luận, chúng tôi phân tích phản ứng bắt xạ pd ở mức năng lượng dưới 300 keV, tập trung vào chuyển dịch lưỡng cực điện (E1). Các trạng thái liên kết và tán xạ được xác định thông qua thế năng Woods-Saxon bằng cách giải các phương trình Schrödinger. Kết quả lí thuyết được so sánh với dữ liệu thực nghiệm chọn lọc để kiểm chứng tính toán lí thuyết của chúng tôi.

Từ khóa: mô hình thế; proton-deuteron; phản ứng bắt xạ